Characterization of Passively Mode-Locked lasers and Saturable Absorbers based on an InP quantum well amplifier suitable for active-passive integration at 1300 nm

Joel Hazan[1], Aser Nassar[1], Steven Kleijn[2], Kevin A. Williams[1], Erwin A.J.M. Bente[1]

[1]Photonic Integration Group, Electrical Engineering department, Eindhoven University of Technology, Groene Loper, Eindhoven, 5600 MB, The Netherlands
[2]Smart Photonics B.V., High Tech Campus, Eindhoven, 5600 MB, The Netherlands

We present the characterization of a two-section Fabry-Perot passively mode-locked laser, with 20 GHz repetition rate, and measurement of the unsaturated absorption of the saturable absorber. The devices have been realized using a new monolithic quantum-well based InP amplifier designed to be included in a photonic integration platform at 1300 nm. Q-switching and mode-locking regimes have been investigated as function of injected current and reverse bias voltage. RF peak power 40 dB over the noise floor and a 12nm broad frequency comb were observed for . The unsaturated absorption of a 100 µm long absorber revealed more than 300 cm^{-1} absorption losses at 1300 nm for -4V of applied reverse bias voltage.

Keywords: *InP, Monolithic Integration, Quantum Wells, Passive Mode-Locking, Semiconductor Lasers, Saturable Absorber,*

INTRODUCTION

The generation of short optical pulses is a key technology in developing ultrafast optoelectronics, and microwave photonics [1], but presents also applications in the distance metrology [2] and in high resolution imaging [3]. Passive mode-locking of laser diodes has been used widely to generate picosecond pulses in the 1300 nm and the 1550 nm wavelength regime [2],[3]. Monolithic passive Mode-Locked lasers (PMLLs) at 1300 nm are often base on quantum dot (QD) laser technology [6], which allows to obtain high pulse power and sub-picosecond pulse durations inside fully active laser systems [7]. The introduction of a new quantum well (QW) based semiconductor optical amplifier (SOA) at 1300 nm, suitable for a generic technology with a butt-joint monolithic active/passive integration scheme [8], leads to the development of QW based extended cavity Mode-locked laser in the 1300 nm wavelength range. Extended cavity designs can lead to higher coherent optical bandwidth and shorter pulse durations [9] due to the possibility to decouple the amplifier and the absorber lengths to the length of the laser cavity which determines the laser repetition rate. In this work we discuss the use of the amplifier developed by us [8] in a fully active Fabry-Perot PMML. The results obtained from the characterization of a PMLL with 20.3 GHz repetition rate are described. Signal to noise ratio of the RF beat signal from the laser of over 40 dB was measured together with a 20 nm wide frequency comb around 1340 nm. Unsaturated absorption measurements to investigate the behaviour of the amplifier under the reverse bias condition and no laser light are also presented. This is intended to be a first step in the realization of extended cavity PMLLs at 1300 nm with active/passive integration capabilities.

PASSIVE MODE-LOCKING

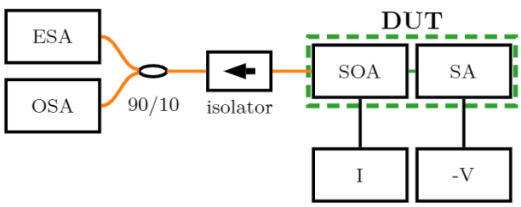

Fig. 1. Schematics of the experimental setup used to characterize the Passively Mode-Locked Lasers

Fully active Fabry-Perot cavity lasers are tested to evaluate the Mode-Locking operation of the quantum well active layers. The longer section that is used as an SOA and is forward biased with a current between 1 and 10 kA/cm^2, while the shorter section is used as a saturable absorber (SA) when reverse biased. The two electrodes are separated by a 20 μm long isolation section where a 1µm of p-doped InP was removed from the waveguide cross section to ensure an electrical resistance between the two electrodes [10]. The chip's uncoated facets reflections are calculated to be 31.7% from simulations. The chip length is 2 mm, which lead to a 20.4 GHz cavity free spectral range. PMLLs with SA lengths of 100 µm and 150 µm have been tested. A schematics of the setup used for the measurements is highlighted in Fig. 1 and briefly described as follows. The light is coupled out from the chip's facet with a lensed single mode optical fiber. After traveling through an optical isolator, which prevents the presence of

any external feedback into the laser cavity, the optical power is detected with an optical (OSA) and an high frequency electrical spectrum analyzer (ESA) connected to a high frequency photodiode (50 GHz). Passive mode-locking (PML) is demonstrated when the SA is reversely biased, and the SOA is forward bias with current injection. Fig. 2. A) shows the radiofrequency (RF) power from the photodiode as a function of current and reverse bias voltage applied to the two-section device. We can notice how the PML at 20.4 GHz happens at higher currents ranging from 100 mA to 115 mA when we increase the SA reverse bias from 0 to -0.7 V. In Fig. 2 b) the PMLL behaviour is depicted as a function of SOA current for a fixed reverse bias voltage of -0.5V. it is possible to identify different operating regimes as function of the injected current between 50 and 200 mA. Above threshold the two section laser operates in a Q-switching regime, i.e. low-frequency self-modulation of the cavity losses [11]. From the 2D map in Fig. 2 b) it is possible to identify the presence of harmonics spaced by 300 MHz around the fundamental frequency of the laser. As we increase the current, those harmonics are translated to sidebands centered to the mode-locking frequency. Further increasing of SOA current above 110 mA leads to mode-locked operation. Fig. 2 c) illustrates the repetition rate frequency tuning to lower frequencies with the current. The tuning of the repetition rate is found to originate from the gain/absorption saturation effects from the cavity's roundtrip frequency in passively mode-locked lasers [1]. We can see how the mode-locking frequency shifts from 20.4 to 20.23 GHz between 110 and 300 mA. At 300 mA, the output optical power on the SA is derived to be as high as 40 mW after subtracting the leakage current from the electrical isolation.

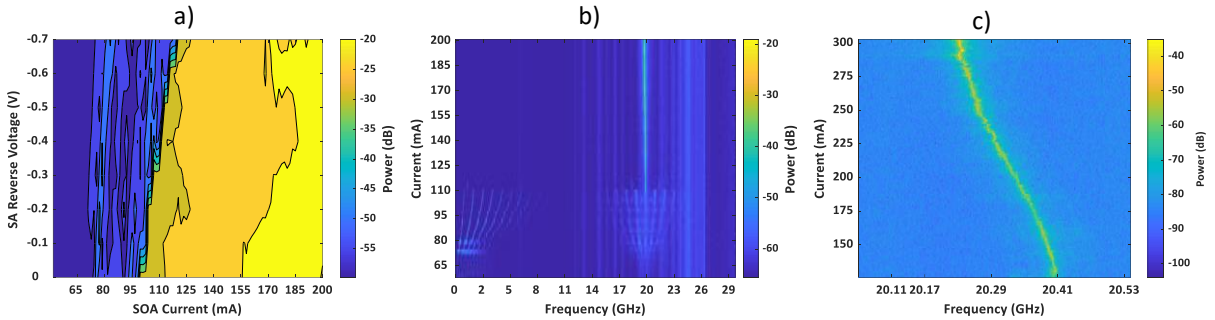

Fig. 2. A) RF Peak Power as function of SOA ($L_{SOA} = 1880\ \mu m$) current and SA ($L_{SA} = 100\ \mu m$) reverse bias voltage. b) 30 GHz RF spectra behaviour as function of SOA current for $V_{Sa} = -0.5V$. c) Details of the RF peak tuning with the SOA current.

The mode-locking behaviour is analysed taking RF spectra with 30 GHz span and 3 MHz resolution as shown in Fig. 3 a). A clear resonance at 20.2 GHz, for an injected current of 270 mA, is shown together with a 40 dB signal to noise ratio. In Fig. 3 b) a 50 KHz resolution scan around 20.3 GHz with a 500 MHz span is presented. The RF linewidth is 4 MHz at -20 dB. A 3 dB linewidth is extracted to be 200 kHz from the linear power scale. Fig. 3 c) depicts an optical spectrum for an operating point of ML operation. It is possible to observe a broadband frequency comb, which is 12 nm within 20 dB below the maximum power, with a full width half maximum (FWHM) of 3 nm around 1340 nm. The frequency comb is shown at higher wavelength compare to the center of the gain spectra of the SOA, (1300 nm at 1 kA/cm^2) as reported in [8], due to the very long SOA and SA sections. Long SOAs allow to have sufficient gain to bleach the SA at around 1340 nm, due to the relatively low absorption of 50 cm^{-1} as shown in Fig. 4 b). This can also explain why in Fig. 2a) the mode-locking threshold current does not vary with the SA reverse bias voltage.

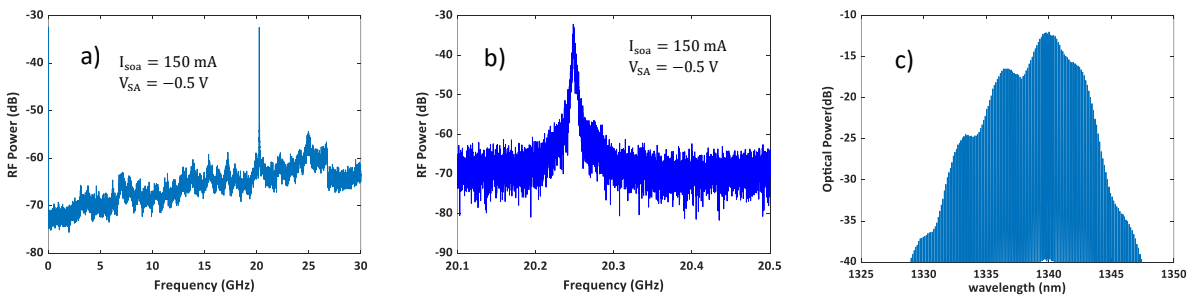

Fig.3. a) RF spectra obtained for a 2 mm long fully active device with L=150 µm absorber reversely biased at V=-0.5V. b) Detail of the RF spectrum around the ML peak. The frequency resolution used in those RF spectra are 3 MHz (a) and 5 kHz (b) respectively. c) Optical spectrum obtained for $I_{soa} = 170$ mA and $V_{sa} = -0.7$ V with a resolution of 1 GHz.

ABSORPTION MEASUREMENTS

The saturable absorber is characterized through unsaturated absorption measurements of the SOA spontaneous emission. The absorption spectrum of a reversely bias SA is calculated from the transmitted power to the SA according to Beer's law as [12]. An anti-reflection (AR) coating is applied to the chip's facets to avoid any lasing behaviour from the two section devices. Fig 4 a) shows the schematics setup used in the absorption measurements.

The optical spectra of the ASE are recorded from both the two edges of the optical chip. We assume that the ASE spectrum generated by the SOA is the same in both directions. So in this way both the input power and the output power which is transmitted through the absorber are recorded. The amplified spontaneous emission is used as input reference power. To ensure an equal amount of coupling losses between the two facets, automated alignment routines are performed to maximize the output power as function of a piezo-controller movement [13]. In Fig. 4 b) the absorption spectra as function of reversely bias applied voltage between -1 and -6V, for a 100 µm long absorber, are plotted. As expected from theory, the absorption decreases at higher wavelengths due to the quantum confined stark effect [14]. Increasing the reverse bias voltage the absorption amplitude increases over the full range due to the voltage dependent carrier extraction from the absorber active region. The increase in the reverse bias induces a frequency shift of the absorption spectra towards shorter wavelength as a result of the electro-absorption. The second decrease in the amplitude of the absorption at low wavelengths (1250 nm) is under investigation. Measurements of polarization resolved absorption are planned to allow us to discriminate between the absorption from an excited state of the quantum wells or from the TM-polarized light absorption, which is shifted in frequency with respect to the TE-polarized light absorption, due to the presence of compressive strain inside the quantum wells, which removes the degeneracy of the light and heavy holes valence energy bands.

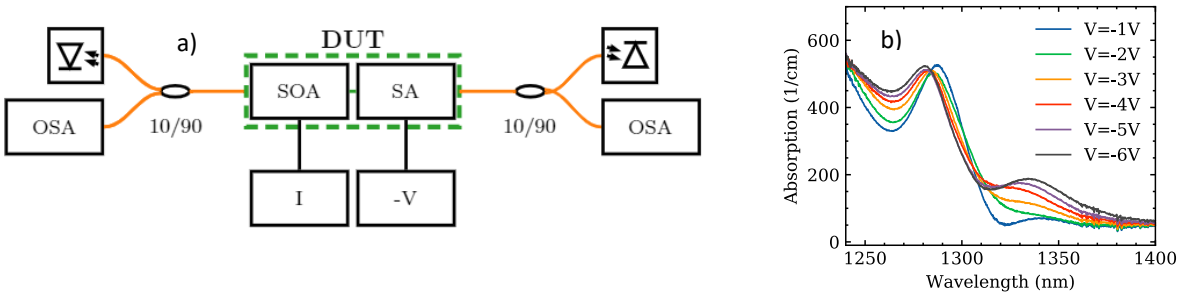

Fig. 4 a) Schematics of the experimental setup used in the optical absorption measurements. b) Absorption spectra for a 100 µm long absorber as function of the reversely bias voltage applied to its contact.

ACKNOWLEDGEMENTS

This publication is part of the project "An integrated Optical Coherence Tomography system for medical imaging at 1300nm" (project number 16251) of the research program HTSM2017 which is (partly) financed by the Dutch Research Council (NWO).

References

[1] S. Arahira and Y. Ogawa, "Repetition-frequency tuning of monolithic passively mode-locked semiconductor lasers with integrated extended cavities," *IEEE J. Quantum Electron.*, vol. 33, no. 2, pp. 255–264, 1997, doi: 10.1109/3.552266.

[2] K. Hei *et al.*, "Distance Metrology with Integrated Mode-Locked Ring Laser," *IEEE Photonics J.*, vol. 11, no. 6, pp. 1–10, 2019, doi: 10.1109/JPHOT.2019.2940068.

[3] W. Drexler, "Ultrahigh-resolution optical coherence tomography," *J. Biomed. Opt.*, vol. 9, no. 1, p. 47, 2004, doi: 10.1117/1.1629679.

[4] G. Carpintero, M. G. Thompson, R. V. Penty, and I. H. White, "Low noise performance of passively mode-locked 10-GHz quantum-dot laser diode," *IEEE Photonics Technol. Lett.*, vol. 21, no. 6, pp. 389–391, 2009, doi: 10.1109/LPT.2008.2011918.

[5] K. A. Williams, M. G. Thompson, and I. H. White, "Long-wavelength monolithic mode-locked diode lasers," *New J. Phys.*, vol. 6, pp. 1–30, 2004, doi: 10.1088/1367-2630/6/1/179.

[6] V. F. Olle, M. G. Thompson, K. A. Williams, R. V. Penty, and I. H. White, "20 GHz picosecond pulse generation by a 1300nm mode-locked quantum dot master oscillator power amplifier," *Conf. Opt. Fiber Commun. Tech. Dig. Ser.*, pp. 2–4, 2009, doi: 10.1364/ofc.2009.owj2.

[7] E. U. Rafailov, M. A. Cataluna, and W. Sibbett, "Mode-locked quantum-dot lasers," *Nat. Photonics*, vol. 1, no. 7, pp. 395–401, 2007, doi: 10.1038/nphoton.2007.120.

[8] J. Hazan, S. Andreou, D. Pustakhod, S. Kleijn, K. Williams, and E. Bente, "1 . 3µm InGaAsP / InP semiconductor optical amplifier compatible with an active / passive integration technology," pp. 5–6, doi: 10.1109/3.283797.A.

[9] V. Moskalenko, S. Latkowski, S. Tahvili, T. de Vries, M. Smit, and E. Bente, "Record bandwidth and sub-picosecond pulses from a monolithically integrated mode-locked quantum well ring laser," *Opt. Express*, vol. 22, no. 23, p. 28865, 2014, doi: 10.1364/oe.22.028865.

[10] J. Hazan, K. A. Williams, and E. A. J. M. Bente, "Gain spectra and saturation power measurements in a two-section InGaAsP / InP semiconductor optical amplifier at 1 . 3 um," *Proc. IEEE Photonics Benelux Symp.*, p. 4, 2021.

[11] E. Bente and M. Smit, "Ultrafast InP optical integrated circuits," *Optoelectron. Integr. Circuits VIII*, vol. 6124, p. 612419, 2006, doi: 10.1117/12.660399.

[12] M. Born and E. Wolf, "Principles of Optics - M.Born, E. Wolf.pdf." 1986.

[13] S. Latkowski, D. Pustakhod, M. Chatzimichailidis, W. Yao, and X. J. M. Leijtens, "Open Standards for Automation of Testing of Photonic Integrated Circuits," *IEEE J. Sel. Top. Quantum Electron.*, vol. 25, no. 5, pp. 1–8, 2019, doi: 10.1109/JSTQE.2019.2921401.

[14] L. A. Coldren, "Diode Lasers and Photonic Integrated Circuits," *Opt. Eng.*, vol. 36, no. 2, p. 616, 1997, doi: 10.1117/1.601191.